

Supplementary Information

1. Electron beam patterning of the Nafion film

The thin Nafion films supported on Au coated silicon wafers were patterned using electron beam lithography as illustrated in Figure S1a. The image also depicts metal marks which were deposited through a stencil mask using electron beam evaporation previous to Nafion spinning. These marks are important to guide the surface focalization when inspecting the film with the optical microscope to estimate EZ. The figure shows the patterned Nafion in a strips (channels) of different lengths. The patterned areas did not exhibit exclusion zones. XPS characterization revealed a significant decrease in the sulfur signal (Fig. S1b) at the e-beam modified area. This finding suggests e-beam induced SO_3^- scission, yielding the loss of Nafion ion-exchange capabilities.

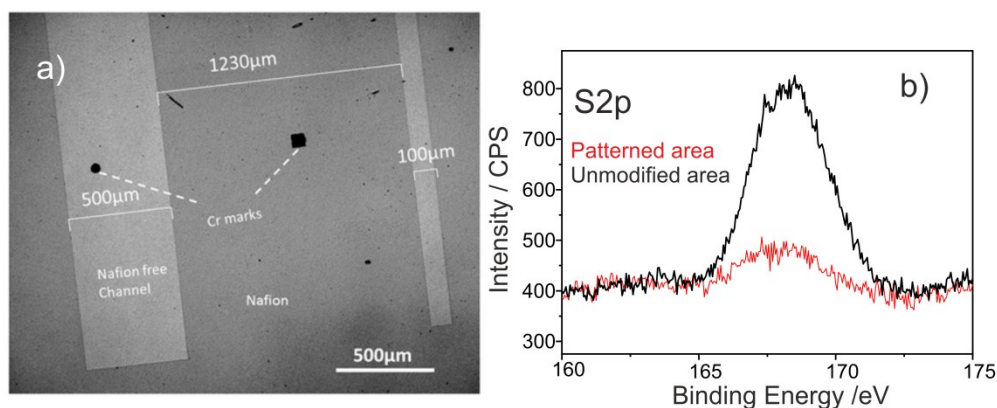


Figure S1. (a) Optical image of a Nafion film with e-beam patterned strips of 500 μm and 100 μm width together with Cr marks. (b) XPS spectra of the S2p signal recorded at the unmodified Nafion area and at the e-beam patterned region.

2. Contact angle of the thin Nafion film

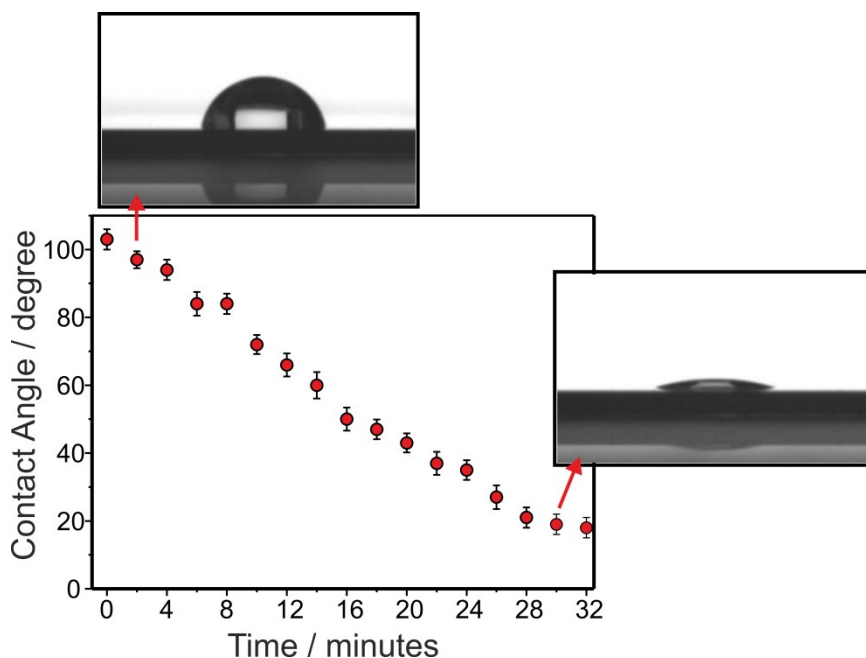


Figure S2. Contact angle measurement of Nafion film as a function of time.

3. Ion exchange capacity measurements

The ion exchange capacity (IEC) was measured by determining the amount of protons released by the thin Nafion film, which was quantified with confocal fluorescence measurements using fluorescent pH indicators. For doing that, the thin Nafion film supported on the Au/Si wafer was incubated overnight in 1M NaCl to induce the proton exchange by Na^+ . Then the pH of the solution was measured using a pH indicator sensitive in the acidic range (LysoSensor yellow/blue DND 160). The measurement was done by exciting at one wavelength (405 nm) and collecting emission around 540 nm. A pH calibration curve was used for extracting the pH of the solution (Fig. S3). Then the IEC was estimated taking into consideration the volume and density of the thin Nafion film ($\text{IEC} = \text{number H}^+ / \text{volume} \times \text{density}$).

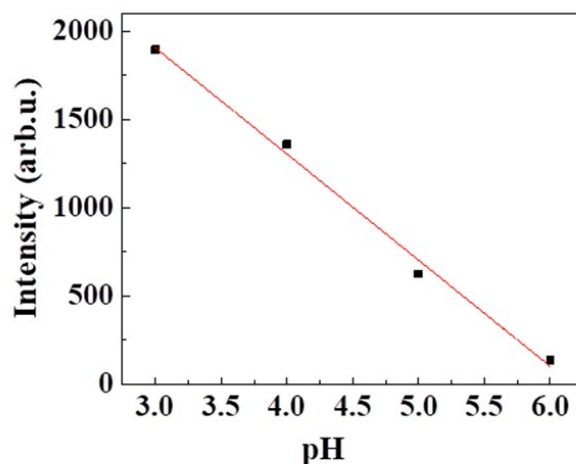


Figure S3. Fluorescence intensity as a function of pH for an excitation wavelength of 405 nm. Black symbols: fluorescence intensity of solutions with known pHs.

4. Schemes of the optical measurement set-up

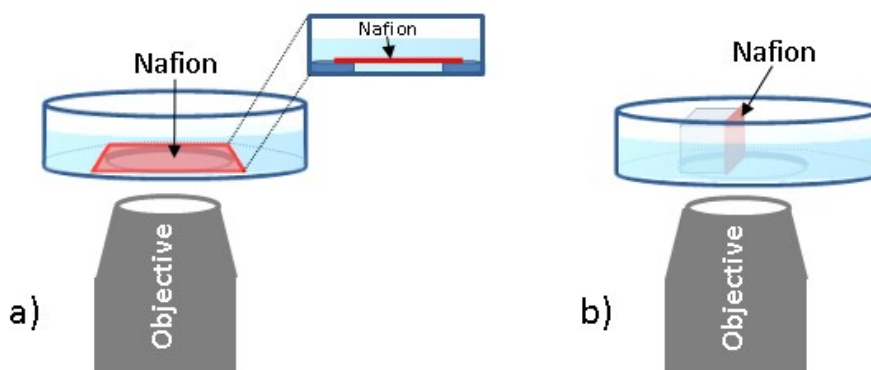


Figure S4. a) Optical measurement set-up for the characterization of the Nafion EZ used in figures 1a-b and 2a. The optical inspection was performed with the Nafion sample on top and the objectives below. b) Optical measurement set-up for a qualitative visualization of the EZ using a confocal fluorescence microscope used for Figures 1d and 2c. The Nafion sample was placed perpendicularly to the microscope objective.

5. Particle sedimentation velocities

The sedimentation velocity for the different particles was obtained by determining the particle distance from the surface of a bare gold sample as a function of time (Fig. S5). Sedimentation velocities of 3.5 $\mu\text{m}/\text{min}$ and 3.6 $\mu\text{m}/\text{min}$ were obtained for plain (left) and carboxylated polystyrene particles (right), respectively.

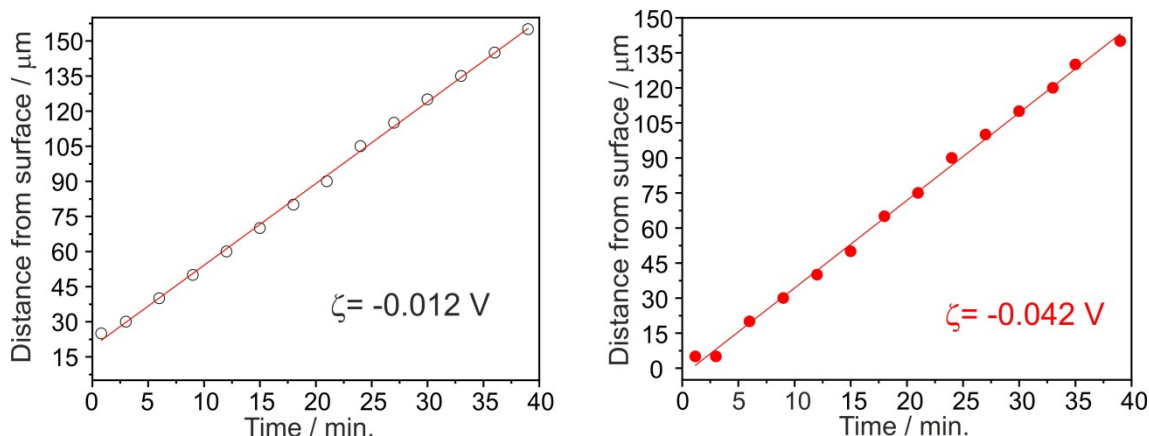


Figure S5. Particle distance from the Au surface as a function of time for the plain ($\zeta = -0.012$ V) and carboxylated particles ($\zeta = -0.042$ V). The sedimentation velocity is obtained as the slope of a linear fit.

6. Effect of salt concentration studied by numerical simulations

A simulation analysis was performed to determine the influence of salt concentration and how it depends on the ion exchange mechanism. Two different sets of boundary conditions were used to evaluate the effect of salt. In the first case, Nafion is considered as a perfect drain for the salt cation, $c_{M^+}(z=0) = 0$. With this boundary condition, the electric field increases with salt concentration up to reach saturation (Figure S6a). In the second case, a first order ion-exchange kinetics was considered and implemented using as a boundary condition, $j_{M^+}(z=0) = -k_{ex}c_{M^+}(z=0)$. In this latter case, the electric field initially increases with salt concentration up to reach a maximum and then decreases at higher concentrations (Figure S6b). The salt concentration values at which the electric field reaches maximum and starts to decrease depend on the value of the reaction rate constant. The electric field starts decreasing at lower salt concentrations if the reaction rate constant becomes lower. Salt-induced electric field screening can be observed with high salt concentrations or with low reaction rate constants, that is, when the ion-exchange mechanism becomes reaction-limited rather than diffusion limited.

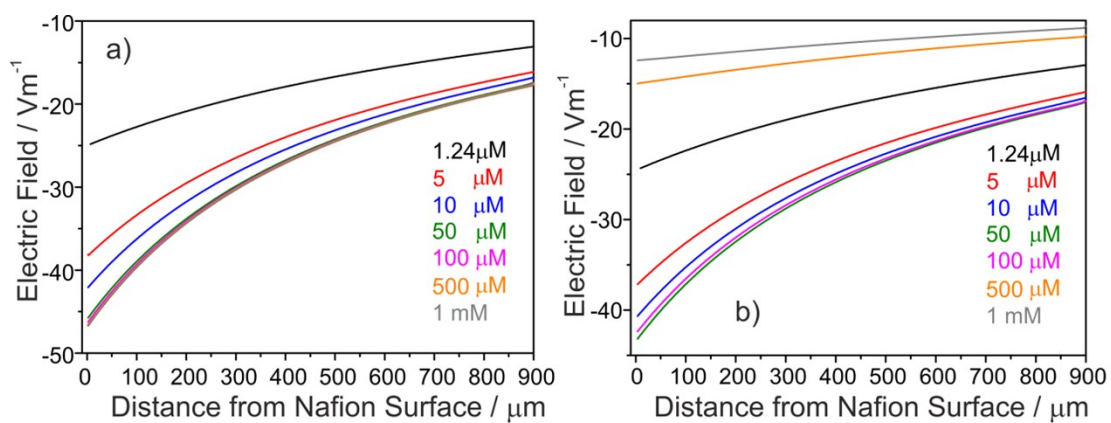


Figure S6. Numerical simulations of the electric field as a function of the distance from Nafion surface in presence of different concentrations of NaCl. (a) Nafion is considered as a perfect drain for the salt cation, (b) the ion-exchange is assumed to be a first order reaction with $k_{\text{ex}}=1 \times 10^{-4}$ m/s.